

Controlled Spacing of Cationic Gold Nanoparticles by Nanocrown RNA

Alexey Y. Koyfman,^{§,†} Gary Braun,[§] Sergei Magonov,[‡] Arkadiusz Chworos,[§] Norbert O. Reich,^{§,†} and Luc Jaeger*^{§,†}

Department of Chemistry and Biochemistry, Biomolecular Science and Engineering Program, University of California - Santa Barbara, Santa Barbara, California 93106-9510, and Veeco Instruments, 112 Robin Hill Road, Goleta, California 93117

Received February 22, 2005; E-mail: jaeger@chem.ucsb.edu

Precise positioning of molecular components for the generation of composite, self-organizing functional devices can be accomplished with nucleic acids due to their defined length, unique base pair recognition capabilities, and possible base and backbone modifications. DNA has been extensively used to control the positioning of proteins¹ and nanoparticles^{2,3} (NP) on the nanoscale,⁴ either by covalent linkages² or electrostatic assembly.³ Various NP/DNA arrangements with geometrical shapes,^{2a-c} straight chains,^{2d} two-dimensional row^{2e} configurations, and their manipulation with enzymes have been described.^{2f,g} As an alternative to DNA, RNA is a promising material for nanoconstruction since it can be manipulated into shapes⁵ more diverse than DNA and can generate high-precision patterns.⁶ Recently, we built a versatile programmable molecular RNA system, called tectosquares (TS), able to assemble into an almost infinite variety of 2D supramolecular architectures^{5,6} that could potentially be used as hosts to precisely organize NPs and other molecular components.

Herein, TS are introduced as the first generation of nanocrown nucleic acids, reminiscent of crown ethers and cryptands.⁷ With their negatively charged, central openings, TS can potentially bind cationic NPs based on electrostatic, size, and shape recognition. In this study, we describe by atomic force microscopy (AFM) the linear arrangement of cationic gold NPs (AuNPs) directed by TS ladders and demonstrate that NP spacing is dependent on the precise architecture of the RNA crown scaffolding.

TS ladder–AuNPs assemblies were hierarchically built in a stepwise fashion (Figure 1). First, two small tectosquares, TS1 and TS2, were formed in the presence of 0.2 mM Mg(OAc)₂ by self-assembly of four different subunits specifically designed to fit each other through loop–loop interactions⁶ (Figure S1). Each subunit comprises a 90° structural motif that promotes the TS square shape. The size of TS was predicted to be ~10 nm with a central opening of ~5 nm by computer modeling (Figures 1 and S1). Due to tip convolution, the TS opening is too small to be resolved by AFM. With a height of 2 ± 0.3 nm and an apparent width of 19 ± 3 nm, TS also appears wider in the AFM images (Figures 2A and S2). TS structural features suggest that a ~5 nm cationic AuNP should be well accommodated within the central TS opening. We synthesized these NPs by coating 3.5 nm gold NPs with a compact ligand shell of 0.7 nm cationic thiocholine, leading to an overall size of ~5 ± 1 nm (Supporting Information and Figure 1). The NPs each have 250–450 positive charges with heights of 4 ± 1 nm and apparent widths of 14 ± 2 nm by AFM analysis (Figures 2B and S3).

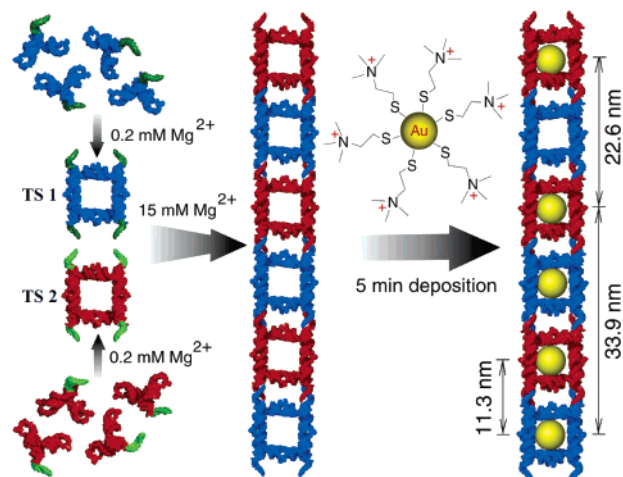


Figure 1. Hierarchical supramolecular assembly of TS ladder decorated with cationic gold NPs. TS1 (blue) and TS2 (red), each made of four different RNA subunits (left), self-assemble through complementary 3' tail–tail connectors (green) into a ladder (center). Once the ladder is formed on the mica surface, cationic, thiocholine-modified gold NPs are electrostatically assembled in solution to the RNA (right). Thiocholines on the gold NP are not to scale. See also Supporting Information.

TS1 and TS2 can further self-assemble hierarchically through complementary tail–tail connectors to form ladders (Figure 1). Three-dimensional (3D) computer modeling predicts the center-to-center distance separating two adjacent TS to be 11.3 nm (Figure 1).

TS1 and TS2 3' tails were designed to promote ladder assembly only upon being mixed. As shown by AFM, neither TS alone generates any supramolecular assemblies (Figures 2A and S2A). However, assembly of an equal amount of TS1 and TS2 in the presence of 15 mM Mg(OAc)₂ led to straight ladders with a height of 1.8 ± 0.2 nm, an apparent width of 17 ± 3 nm, and lengths ranging from 42 to 388 nm that correspond to 4–33 TS joined together (Figures 2C and S2B).

After TS ladder assembly and deposition on mica, subsequent treatment for 5 min with the cationic AuNPs showed the resultant TS ladder–AuNP assemblies to have a height of 4 ± 1 nm, twice as tall as undecorated TS ladders, and lengths ranging from 50 to 400 nm (Figures 2D and S4). The majority of the NPs along the RNA ladder had peak-to-peak separations of 11.8 ± 1.6 nm (*n* = 222), while the remaining NP separations were either 2 or 3 times longer (22.9 ± 2.1 nm (*n* = 127); 33.6 ± 2.0 nm (*n* = 31)), strongly suggesting that the RNA ladder was directing the positioning of the ~5 nm AuNPs (Figures 2D, 3, and S4). The average separation distance between NPs depends on the NP concentration (data not shown). However, high ratios of NPs to TS ladders favor NP spacing of ~11.8 nm, whereas lower ratios favor the larger

[§] Department of Chemistry and Biochemistry, University of California - Santa Barbara.

[†] Biomolecular Science and Engineering Program, University of California - Santa Barbara.

[‡] Veeco Instruments.

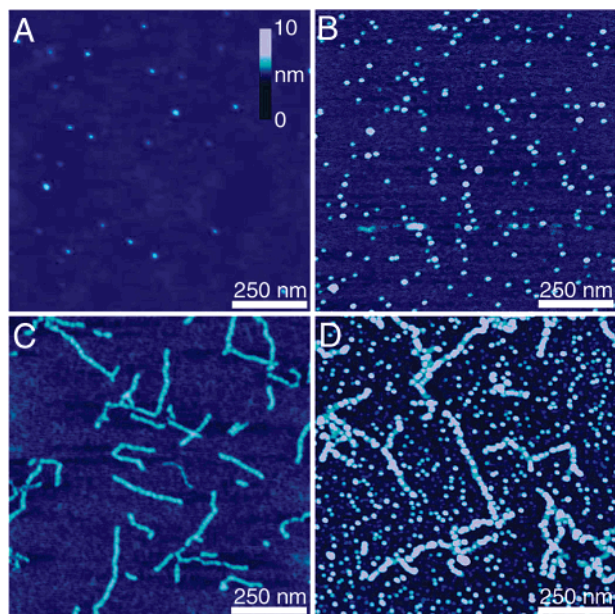


Figure 2. AFM images of TS RNA ladders decorated with gold NPs. (A) TS1 alone. (B) cationic gold NPs alone, (C) TS1–TS2 ladder, (D) TS1–TS2 RNA ladder decorated with cationic gold NPs. Vertical scale bar is 10 nm for all images. Same [RNA] were deposited on the mica surface. Variation in the observed numbers of TS (2A) and ladders (2C) most likely derives from the relative ability of each TS to be retained on the mica surface compared to the ladder (Supporting Information).

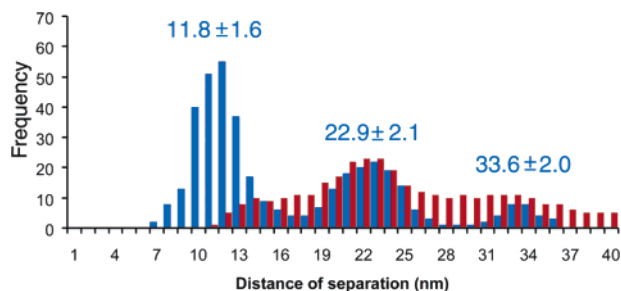


Figure 3. Distributions of distance separating adjacent gold NPs along TS RNA ladder (blue, $n = 380$) and duplex DNA (red, $n = 330$).

separations. By contrast, NPs bound along linear stretches of duplex DNA³, which also utilize electrostatic attractions for their assembly, had much less defined spacing. In the DNA/NP system, the separation between two NPs ranged from 12 to 40 nm over 330 distance measurements with a small peak at 22 nm^{3d} (Figure 3). As mentioned in earlier studies³, the spacing statistics for solution-based assembly of cationic NPs and long dsDNA strands appear to be controlled by ligand shell sterics and electrostatics.

The observed spacing of gold NPs along TS ladders is in remarkable agreement with the model predicting an interparticle distance of 11.3 nm if NPs are bound in TS openings (Figures 1 and 3). Thus, we propose that the special geometry of the TS ladder guides the positioning of cationic gold NPs by favoring their binding to the central opening of TS units, maximizing the number of interactions between the positive thiocholines and the negative RNA backbone, while minimizing electrostatic repulsion between adjacent gold NPs. Indeed, ~5 nm NPs binding to the TS centers can potentially interact with 30–40 phosphates, while those binding

to exteriors or corners of TS can only bind 7–14 phosphates, as they would do with the DNA duplex.

We anticipate that TS can be designed to direct the assembly of many other NPs. As nanocrown RNA, the size of the structure and the number of phosphates in the inner part of the TS as well as the size composition and surface chemistry of the NP should determine the stability of the RNA/NP complexes. For instance, the positioning of these ~5 nm cationic NPs onto ladders made of larger TS in which the central opening is ~8 nm did not produce any well-defined spacings (data not shown). Alternatively, modified RNA nucleotides and backbone modifications can potentially be used to further control the assembly of NPs.

Nanodevices with semiconducting or magnetic properties⁹ that take advantage of RNA scaffoldings to achieve precise control over the positioning of NPs could potentially find applications in nanoelectronics⁴ or medicine.¹⁰

Acknowledgment. Thanks to I. Severcan for RNA preparation and C. Geary for assistance with RNA modeling. We are grateful to the NSF (CHE-0317154 and MRSEC DMR00-80034, L.J.) and to the ICB (DAAD19-03-D-0004, N.O.R.) for financial support. This work made use of MRL Central Facilities at UCSB.

Supporting Information Available: Materials and methods and supporting figures. This material is available free of charge via the Internet at <http://pubs.acs.org>.

References

- (1) Yan, H.; Park, S. H.; Finkelstein, G.; Reif, J. H.; LaBean, T. H. *Science* **2003**, *301*, 1882–1884.
- (2) (a) Alivisatos, A. P.; Johnsson, K. P.; Peng, X.; Wilson, T. E.; Loweth, C. J.; Bruchez, M. P.; Schultz, P. G. *Nature* **1996**, *382*, 609–611. (b) Loweth, C. J.; Caldwell, W. C.; Peng, X.; Alivisatos, A. P.; Schultz, P. G. *Angew. Chem., Int. Ed.* **1999**, *38*, 1808–1812. (c) Zanchet, D.; Micheel, C. M.; Parak, W. J.; Gerion, D.; Williams, S. C.; Alivisatos, A. P. *J. Phys. Chem. B* **2002**, *106*, 11758–11763. (d) Le, J. D.; Pinto, Y.; Seeman, N. C.; Musier-Forsyth, K.; Taton, T. A.; Kiehl, R. A. *Nano Lett.* **2004**, *4*, 2343–2347. (e) Li, H.; Park, S. H.; Reif, J. H.; LaBean, T. H.; Yan, H. *J. Am. Chem. Soc.* **2004**, *126*, 418–419. (f) Kanaras, A. G.; Wang, Z.; Bates, A. D.; Cosstick, R.; Brust, M. *Angew. Chem., Int. Ed.* **2003**, *42*, 191–194. (g) Yun, C. S.; Khitrov, G. A.; Vergona, D. E.; Reich, N. O.; Strouse, G. F. *J. Am. Chem. Soc.* **2002**, *124*, 7644–7645. (h) Medalia, O.; Heim, M.; Guckenberger, R.; Sperling, R.; Sperling, J. *J. Struct. Biol.* **1999**, *127*, 113–119.
- (3) (a) Woehrl, G. H.; Warner, M. G.; Hutchison, J. E. *Langmuir* **2004**, *20*, 5982–5988. (b) Wang, G.; Murray, R. W. *Nano Lett.* **2004**, *4*, 95–101. (c) Warner, M. G.; Hutchison, J. E. *Nat. Mater.* **2003**, *2*, 272–277. (d) Braun, G.; Inagaki, K.; Estabrook, R. A.; Wood, D.; Levy, E.; Cleland, A.; Reich, N. O. Manuscript submitted.
- (4) (a) Seeman, N. C. *Nature* **2003**, *421*, 427–431. (b) Chung, S.-W.; Ginger, D. S.; Morales, M. W.; Zhang, Z.; Chandrasekhar, V.; Ratner, M. A.; Mirkin, C. A. *Small* **2005**, *1*, 64–69.
- (5) (a) Westhof, E.; Masquida, B.; Jaeger, L. *Folding Des.* **1996**, *1*, R78–R88. (b) Jaeger, L.; Westhof, E.; Leontis, N. B. *Nucleic Acids Res.* **2001**, *29*, 455–463. (c) Jaeger, L.; Leontis, N. B. *Angew. Chem., Int. Ed.* **2000**, *39*, 2521–2524. (d) Liu, B.; Baudrey, S.; Jaeger, L.; Bazan, G. C. *J. Am. Chem. Soc.* **2004**, *126*, 4076–4077. (e) Shu, D.; Moll, W.; Deng, Z.; Mao, C.; Guo, P. *Nano Lett.* **2004**, *4*, 1717–1723. (f) Ikawa, Y.; Tsuda, K.; Matsumura, S.; Inoue, T. *Proc. Natl. Acad. Sci. U.S.A.* **2004**, *101*, 13750–13755.
- (6) Chworos, A.; Severcan, I.; Koefman, A. Y.; Weinkam, P.; Oroudjev, E.; Hansma, H. G.; Jaeger, L. *Science* **2004**, *306*, 2068–2072.
- (7) Gokel, G. W.; Leevy, W. M.; and Weber, M. E. *Chem. Rev.* **2004**, *104*, 2723–2750.
- (8) Sheiko, S. S.; Moller, M. *Chem. Rev.* **2001**, *101*, 4099–4124. Hansma, H. G.; Oroudjev, E.; Baudrey, S.; Jaeger, L. *J. Microsc.* **2003**, *212*, 273–279.
- (9) Moser, A.; Takano, K.; Margulies, D. T.; Albrecht, M.; Sonobe, Y.; Ikeda, Y.; Sun, S.; Fullerton, E. E. *J. Phys. D: Appl. Phys.* **2002**, *35*, R157–R167.
- (10) Michalek, X.; Pinaud, F. F.; Bentolila, L. A.; Tsay, J. M.; Doose, S.; Li, J. J.; Sundaresan, G.; Wu, A. M.; Gambhir, S. S.; Weiss, S. *Science* **2005**, *307*, 538–544.

JA051144M